A State Parameter Modified Drucker-Prager Cap Model

Farzad Eskandari
Graduate Student, Faculty of Engineering, Memorial University of Newfoundland, St. Johns, Canada
Ryan Phillips
Principal Consultant, C-CORE, Memorial University of Newfoundland, St. Johns, NL, Canada
Bipul Hawlader
Associate Professor, Faculty of Engineering, Memorial University of Newfoundland, St. Johns, NL, Canada

ABSTRACT
A variant of the Drucker-Prager Cap model is developed to more realistically capture the behaviour of sand under large deformation. The initiative of this work comes from the need to develop a user defined constitutive model in ABAQUS Explicit v6.7 finite element software. The model has been developed to resolve the existing issues of dilation rates of built-in models in ABAQUS. The classic Drucker-Prager model with or without a cap which are widely used in modeling of sand can lead to excessive dilation. The control and suppression of dilatancy is essential when the soil undergoes very large plastic deformation. The proposed model introduces a dilation rate in accordance with experimental correlations based on the Bolton stress dilatancy relationship. A hardening law consistent with the critical state soil mechanics concept is also proposed. The evolution of yield surface controls and limits the dilation of the soil. The proposed model requires a total of ten input parameters, which can be obtained from conventional laboratory tests. The performance of the model has been validated with the triaxial test results under drained conditions.

RÉSUMÉ
Une variante du modèle de Drucker-Prager Cap est mise au point pour capturer de façon plus réaliste le comportement des sables sous d'importantes déformations. L'initiative de ce travail vient de la nécessité d'élaborer un modèle de comportement défini par l'utilisateur dans ABAQUS Explicit v6.7. Ce modèle est développé afin de résoudre les problèmes existants des taux de dilatation des modèles encastrables. Le modèle classique de Drucker-Prager avec ou sans capuchon, qui sont largement utilisés dans l'analyse numérique des sols peut conduire à une dilatation excessive. Le contrôle et la suppression de dilatance est essentiel lorsque le sol est soumis à de grandes déformations plastiques. Le modèle proposé introduit un taux de dilatation conformément aux corrélations expérimentales basées sur la relation contrainte-dilatation de Bolton. Une loi de durcissement compatible avec les concepts de mécanique des sols à l'état critique est ajouté. L'évolution des surfaces de rendement contrôle et limite la dilatation du sol. Le modèle constitutif proposé est simple à calibrer avec un total de dix paramètres qui peuvent être obtenue à partir de test conventionnels en laboratoire. Le modèle est validé avec les résultats des essais triaxiaux en conditions drainées.

1 INTRODUCTION

Existing soil constitutive models are relatively simplistic for use in finite element analyses based on single phase explicit formulation used with adaptive meshing. More sophisticated models are needed to correctly capture the behaviour of soil, for example the seabed response to ice gouging where seabed shear strains could be up to 1000% as shown in Figure 1 (Phillips *et al.* 2010). ABAQUS Explicit v6.7 allows users to develop their own material models and enhance the explicit analyses by implementation of user defined material subroutine VUMAT. This feature in ABAQUS is helpful in problems like ice gouging where the built-in models have a number of limitations.

The coupled effects of density and confining pressure on soil behaviour have been studied by a number of researchers (e.g. Roscoe and Poorooshasb 1963; Been and Jefferies 1985; Bolton 1986; Ishihara 1993; and Verdugo 1992). One common point is that in each of these studies an index was defined to describe the effects of initial state of sand on stress-strain behaviour. The index is a measure of the distance between initial state and ultimate state where the failure occurs. It has been shown that these indices better represent the soil state and stress-stain behaviour than the relative density (D_r) generally used in geotechnical engineering (Cubrinovski and Ishihara, 1998).

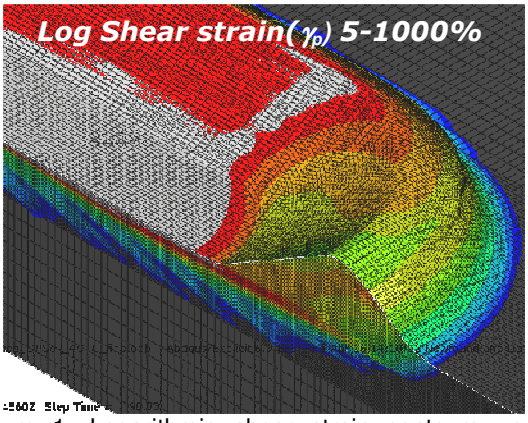

Figure 1. Logarithmic shear strain contours under a gouging ice keel

Proper simulation of dilatancy rate is an essential part of a constitutive model of granular soil. Vermeer and de Borst (1984) reported typical values of dilation angles of various soils, which have been widely used as input in constitutive models. Bolton (1986) also proposed a relationship for the maximum dilation angle based on available test data.

Another critical aspect in modeling of sand behaviour is the selection of appropriate yield surface. While the Drucker-Prager criterion (Drucker and Prager 1952) is frequently used in modeling of sand, one of the major limitations in the Drucker-Prager yield surface with an associated flow rule is that it results a dilatancy rate that is considerably higher than the values observed in reality. In addition, because the yield surface is not closed along the hydrostatic pressure (p') axis in p'-q space, the prediction may not be realistic in compression. In order to overcome these deficiencies, Drucker *et al.* (1957) added a cap for compression yield which could harden or softens with plastic strain.

The objective of this study is to develop a new method to control excessive dilation of dense sand using a non-associated flow rule. The paper consists of four parts. The first part shows the performance of Bolton's (1986) dilatancy relationships comparing with updated laboratory test results available in the literature. The second part deals with the model formulation. The numerical code is used to show the performance of the model comparing the results with available test data in the third part. Finally, a parametric study has also been performed in order to show the effects of some critical input parameters.

2 DILATANCY RELATION

Bolton (1986) proposed the *Dilatancy Index* (I_R) as:

$$I_R = I_D\left(Q - \ln p'\right) - 1 \qquad [1]$$

where I_D is the relative density which can be expressed as:

$$I_D = \frac{e_{\max} - e}{e_{\max} - e_{\min}} \qquad [2]$$

where e_{max} and e_{min} are the maximum and minimum void ratios, respectively; e is the current void ratio; p' is the mean effective stress in kPa; and Q is a fitting parameter. Bolton (1986) showed that Q = 10 gives an adequately good fit for triaxial and plane strain test data considered in his study. However, Chakraborty and Salgado (2010) suggested that in order to achieve more realistic results at low pressures Q should be written as:

$$Q = 7.4 + 0.6\ln p' \text{[kPa]} \qquad [3]$$

Dilatancy rate at peak of stress-strain curve (D_B^p) can be written as (Bolton, 1986):

$$D_B^p = -\frac{d\varepsilon_v}{d\varepsilon_1} = 0.3I_R \qquad [4]$$

where ε_v is the volumetric strain and ε_1 is the major principal strain. The subscript *B* means that the dilatancy rate is based on the Bolton relationship.

The strain variables in the triaxial space are defined as:

$$\varepsilon_v = \varepsilon_1 + 2\varepsilon_3 \qquad [5]$$

$$\varepsilon_q = \frac{2}{3}\left(\varepsilon_1 - \varepsilon_3\right) \qquad [6]$$

where subscripts 1 and 3 correspond to axial and radial directions and subscript v and q are respectively the volumetric and deviatoric strain components.

The total strain consists of elastic and plastic components. However, at the peak stress level the elastic component of strain is negligible to plastic component (Jefferies, 1997). Therefore, neglecting the elastic component of strain at the peak and using Eqs [4], [5] and [6] the dilatancy rate at the peak (D^p) for triaxial stress space can be written as:

$$D^p = -\frac{d\varepsilon_v^p}{d\varepsilon_q^p} = \frac{3D_B^p}{3 + D_B^p} \qquad [7]$$

Jefferies and Been (2006) compiled a large number of triaxial test data on various sands available in the literature. In this study a total of 203 tests results are considered as the required information is available. Figure 2 shows a comparison between measured and predicted dilatancy rate using Eq. 7. Note that, the value of D^p obtained from Eq. 7 is positive. However, in order to be consistent with Jefferies and Been (2006), where the dilation rate at the peak has been reported as minimum value, D^p has been shown with a negative sign in Figure 2. The identical solid line is drawn to compare measured and predicted dilatancy rates. As shown, Eq. 7 predicts the dilation rate reasonably well considering the fact that there is a wide variation in these tests such as specimen preparation, loading, saturation and others.

Bolton (1986) also proposed a relationship between the angles of internal friction at peak stress (ϕ'_{max}) and at critical stress (ϕ'_{cr}), and dilatancy index (I_R) as:

$$\phi'_{\max} = \phi'_{cr} + 3I_R \qquad [8]$$

Figure 3 shows the comparison between the measured values (Jefferies and Been, 2006) and predictions using Eq. 8. A total of 165 triaxial test results are plotted in this figure. A reasonably good comparison was also found for angle of internal friction.

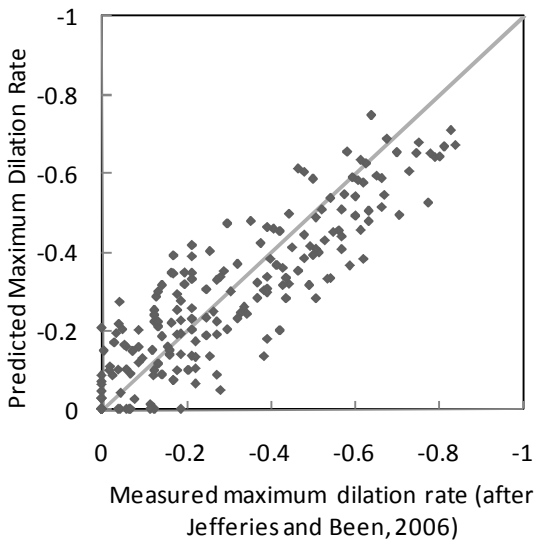

Figure 2. Dilatancy rate at peak stress

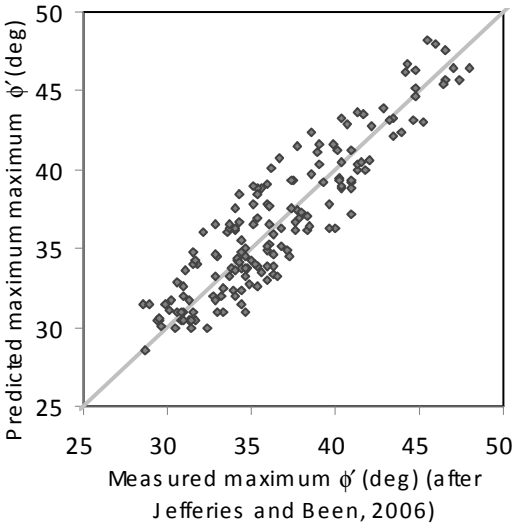

Figure 3. Predicted ϕ'_{max} using Bolton's dilatancy index against measured test data

3 MODEL FORMULATION

The proposed model includes the three fundamental elements as described in Sections 3.1 - 3.3.

3.1 Yield Surface

The yield function is defined using Drucker-Prager Cap model, which consists of three surfaces shown in Figure 4. These surfaces are the shear surface, transition surface and a cap. The shear surface defines the region where the failure is dominant by shear flow while the cap accounts mainly the plastic compaction behaviour. The transition surface is implemented in order to avoid numerical instability. This surface provides a smooth transition from the shear zone to the cap. These three surfaces can be defined as:

For shear surface AB (i.e. $p' \le p_a - A\gamma\sin\theta$)

$$F_s = q - p'\tan\theta - d \quad [9]$$

On the cap CD (i.e. $p' \ge p_a$)

$$F_c = \left(\frac{p'-p_a}{B}\right)^2 + \left(\frac{q}{A(1+\gamma-\gamma/\cos\theta)}\right)^2 - 1 \quad [10]$$

On the transition zone BC (i.e. $p_a - A\gamma\sin\theta < p' < p_a$)

$$F_t = q - (1-\gamma/\cos\theta)A - \sqrt{(A\gamma)^2 - (p'-p_a)^2} \quad [11]$$

where p' is the mean effective stress; q is deviatoric stress; γ is the radius of the transition surface; p_a is an evolution parameter which controls the size of the yield surface; A and B are respectively vertical and horizontal radii of the cap; θ is the slope of the shear failure line in p'-q space; and d is the cohesion intercept.

The values of θ and d could be obtained from effective strength parameters ϕ' and c'.

$$\theta = \frac{2\sin\phi'}{\sqrt{3}(3-\sin\phi')} \quad [12]$$

$$d = \frac{6c'\cos\phi'}{\sqrt{3}(3-\sin\phi')} \quad [13]$$

Also:

$$A = d + p_a\tan\theta \quad [14]$$

$$B = RA \quad [15]$$

where R is the cap eccentricity parameter

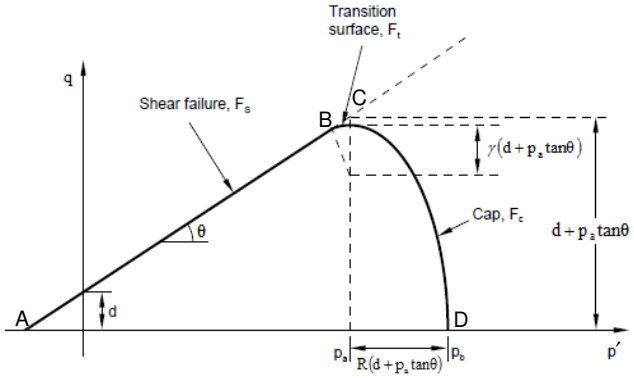

Figure 4. Drucker-Prager Cap yield surface

3.2 Plastic Potential Function

In this study, the flow rule is assumed to be associated on the cap and non-associated on shear and transition surfaces. The following plastic potential

function has been used for the shear and transition zones.

$$G_{st} = \left(\frac{p' - p_a}{\beta} \right)^2 + \left(\frac{q}{\alpha(1 + \gamma - \gamma/\cos\theta)} \right)^2 - \varepsilon \quad [16]$$

where α and β are respectively the vertical and horizontal radii of the ellipse of the plastic potential function in shear and transition zones and ε is a constant. The subscripts *st* represents that Eq. 16 is applicable to both shear and transition zones.

From some geometric relationships, α and β can be found as:

$$\alpha = d + p_a \tan\theta \quad [17]$$

$$\beta = d/\tan\theta + p_a \quad [18]$$

3.3 Hardening Law

The third fundamental element of the model is the hardening law which has been defined based on the critical state soil mechanics concepts as:

$$dp_a = H(p_{a,\max} - p_a)d\varepsilon_q^p \quad [19]$$

$$d\theta = H(\theta_{\max} - \theta)d\varepsilon_q^p \quad [20]$$

where *H* is the hardening modulus; $p_{a,max}$ is the maximum value of the evolution parameter p_a; and θ_{max} is the maximum value of θ. In this model, $p_{a,max}$ and θ_{max} limit the size of the yield surface resulted from strain hardening. As shown later, the value of $p_{a,max}$ and θ_{max} are determined based on the dilatancy index (I_R) using current value of p' and I_D.

It is to be noted here that Eqs. 19 and 20 present a simple hardening law which is in agreement with critical state soil mechanics concepts and restricts the size of the yield surface to a maximum allowable value based on the state of the soil. These equations are functions of plastic shear strains.

Following Jefferies and Been (2006), Eq. 19 can be written in a dimensionless form as:

$$\frac{dp_a}{p'} = H\left[\left(\frac{p_a}{p'} \right)_{\max} - \frac{p_a}{p'} \right] d\varepsilon_q^p \quad [21]$$

For triaxial condition θ_{max} can be expressed in terms of ϕ'_{max} as:

$$\theta_{\max} = \tan^{-1}\left(\frac{6\sin\phi'_{\max}}{3 - \sin\phi'_{\max}} \right) \quad [22]$$

As the soil elements are assumed to obey the normality rule, the plastic strain increments can be calculated as:

$$d\varepsilon_v^p = \chi \frac{\partial G}{\partial p} \quad [23]$$

$$d\varepsilon_q^p = \chi \frac{\partial G}{\partial q} \quad [24]$$

where χ is a scalar multiplier and *G* is the plastic potential surface.

Now substituting $d\varepsilon_v^p$ and $d\varepsilon_q^p$ from Eqs. 23 and 24 into Eq. 7 and then using θ_{max} from Eq. 22 the following equation can be obtained.

$$\left(\frac{p_a}{p'} \right)_{\max} = 1 + \frac{D^p}{\tan\theta_{\max}} \quad [25]$$

Eq. 25 defines the ratio of evolution parameter to the mean stress at the peak state. Note that *d*=0 for sand.

3.4 Dilation Limit

The Drucker-Prager plastic potential function generally results in an excessive amount of dilation in shear at relatively low confining pressures. This is attributed to the nearly horizontal normal vectors on the ellipse of plastic potential function at lower values of p', which results in larger volumetric strain increments and thereby higher dilatancy rate. In order to avoid this problem a modified plastic potential surface in the shear zone is proposed to limit the dilatancy to a specified value. In this paper the maximum dilation suggested by Bolton (1986) which is presented in Eq. 7 is selected as the limiting dilation rate. Therefore, for each plastic potential surface in p' - q space a transition mean pressure $p_{D^p_{\max}}$ can be obtained by substituting $d\varepsilon_v^p$ and $d\varepsilon_q^p$ from Eqs. 23 and 24 into Eq. 7.

$$p_{D^p_{\max}} = \frac{p_a \tan^2\theta - D^p_{\max} d}{D^p_{\max} \tan\theta + \tan^2\theta} \quad [26]$$

That means the plastic potential function for mean stress less than $p_{D^p_{\max}}$ is a straight line (Figure 4). However, the plastic potential function for a mean stress between $p_{D^p_{\max}}$ and p_a remains the same as Eq. 16.

During shearing the value of $p_{D^p_{\max}}$ is changing because I_R is a function of current state of stress and density. Therefore, the shape of the plastic potential function should be updated with progress of shearing.

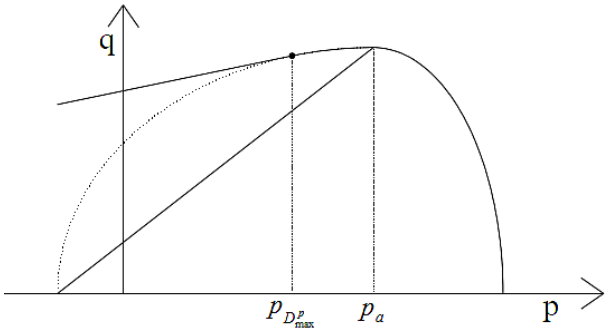

Figure 5. Two segmented plastic potential function in shear zone

4 MODEL VALIDATION

The proposed model is used to simulate some triaxial test results of sand samples under different loading and initial conditions (Jefferies and Been, 2006). A total of 10 input parameters are required for this model, which are module of elasticity E, Poisson's ratio ν, cohesion intercept d, the slope of the failure line θ_{cr}, evolution parameter p_a, minimum void ratio e_{min}, maximum void ratio e_{max}, void ratio e, hardening modulus H and eccentricity parameter R. The parameters used in these analyses are listed in Table 1. The value of θ_{cr} is obtained from the plot of respective test data in p' - q space. Since the analysis has been performed only for sand, d = 0 is used. The elastic modulus E, hardening modulus H and cap eccentricity R have been estimated based on density and confining stress of the specimen. The value of Poisson's ratio ν = 0.2 is adopted.

Figures 6 and 7 show the simulation of dense Erksak sand and in Figures 8 and 9 the response of loose Erksak sand is predicted using the constitutive model. Figure 10 shows the simulation results of triaxial test of dense Ticinio sand.

As shown, the proposed model reasonably predicts the test results.

Table 1. Model input parameters

	Erksak 330/7 (Fig.5)	Erksak 330/7 (Fig.6)	Erksak 330/7 (Fig.7)	Erksak 330/7 (Fig.8)	Ticinio 530/0 (Fig.9)
E(kPa)	$2.07x10^5$	$2.0x10^5$	$1.07x10^5$	$5.75x10^4$	$8.0\ x10^5$
v	0.2	0.2	0.2	0.2	0.33
θ_{cr} (deg)	52	53	49	49	54
e_{max}	0.747	0.747	0.747	0.747	0.89
e_{min}	0.521	0.521	0.521	0.521	0.6
e	0.59	0.667	.775	0.82	0.66
H	300	200	55	75	150
R	2.5	2.5	1.2	1.2	3
p_0 (kPa)	130	60	1000	200	100

The value of p_a is derived according to p_0, R and θ

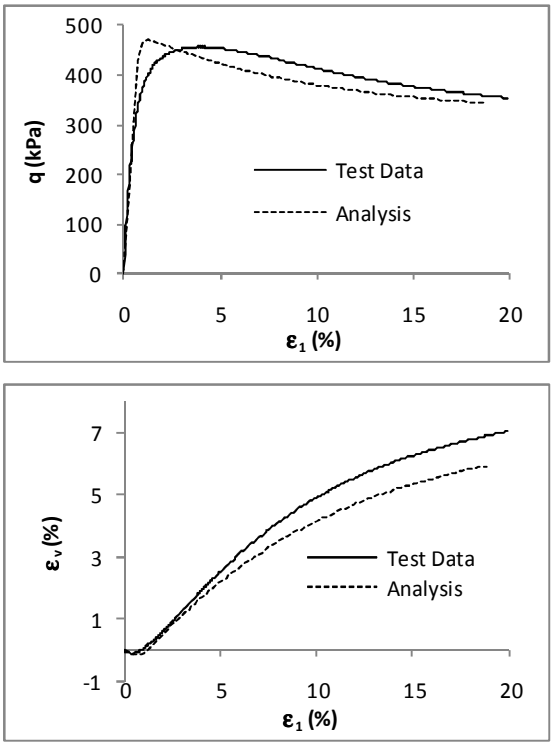

Figure 6. Simulation of drained triaxial test of a dense sample of sand (Erksak 330/7, e_0 = 0.59, p_0 = 130 kPa)

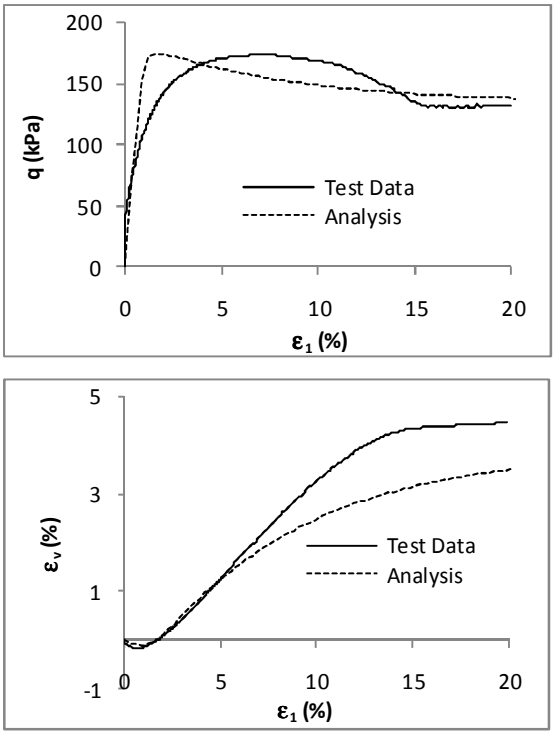

Figure 7. Simulation of drained triaxial test of a dense sample of sand (Erksak 330/7, e_0 = 0.677, p_0 = 60 kPa)

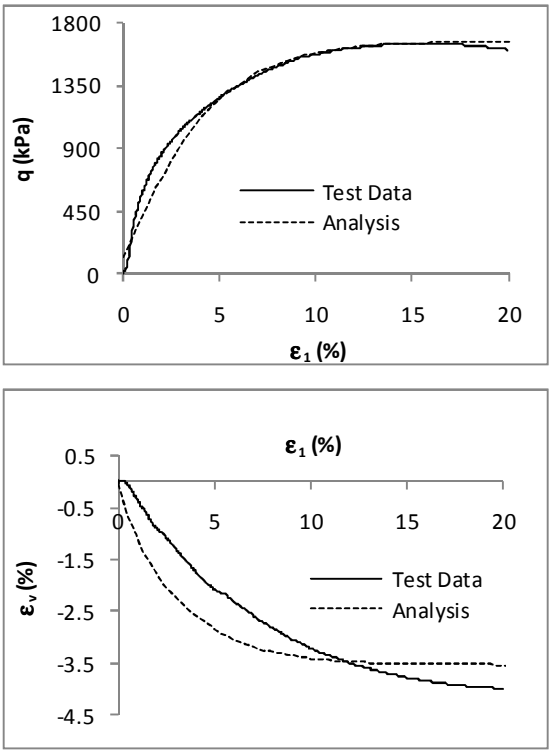

Figure 8. Simulation of drained triaxial test of a loose sample of sand (Erksak 330/7, e_0 = 0. 775, p_0 = 1000 kPa)

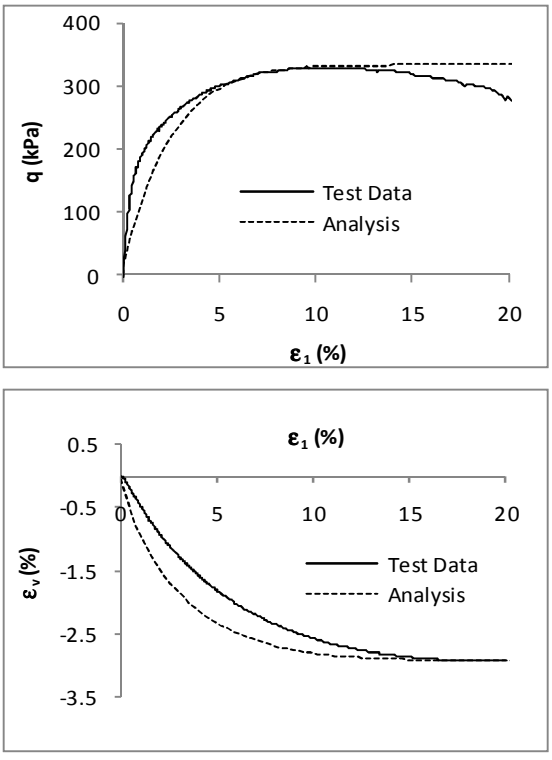

Figure 9. Simulation of drained triaxial test of a loose sample of sand (Erksak 330/7, e_0 = 0.82, p_0 = 200 kPa)

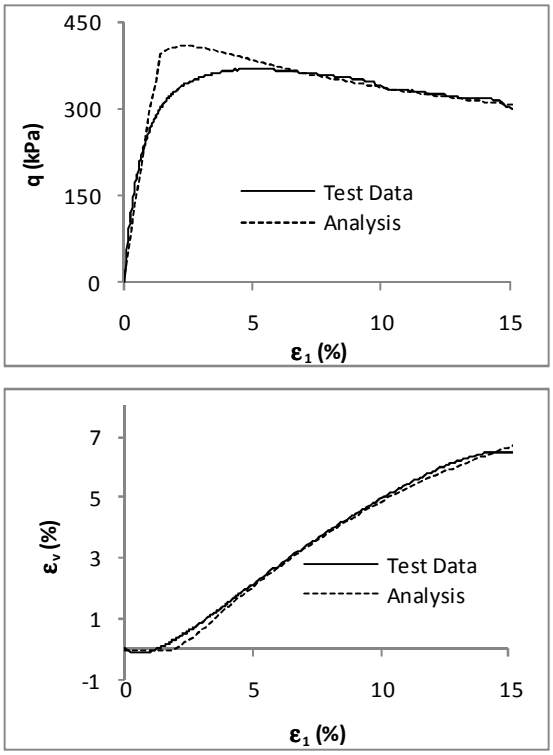

Figure 10. Simulation of drained triaxial test of a dense sample of sand (Ticinio 530/0, e_0 = 0.66, p_0 = 100 kPa)

5 PARAMETERIC STUDY

In this section the model sensitivity to the variation of input parameters is investigated. The parameters used in baseline analysis are shown in Table 2. The parametric study is performed for four critical parameters (E, θ, D_r and H) which have significant influence on model performance. The parametric study has been carried out by varying one parameter at a time while keeping all other parameters at the same value as that of the baseline analysis (Table 2). Figures 11 to 14 show the predicted results for various conditions. One line in these figures show the baseline analysis while the other two lines show the effects of corresponding input parameters.

Table 2. Model parameters for sensitivity analysis

E	2.07×10^5 kPa	D_r	60%
v	0.2	H	150
d	0	R	2.5
θ_{cr}	52°	e_0	0.58

From ε_q vs. ε_v plots it is realized that the predicted dilatancy rate (i.e. slope of the curve) using the proposed model is zero at high strain level (e.g. $\varepsilon_q^p > 50\%$). This feature is important in large deformation problems such as ice gouging where shear strains could be even more than 1000% as shown in Figure 1.

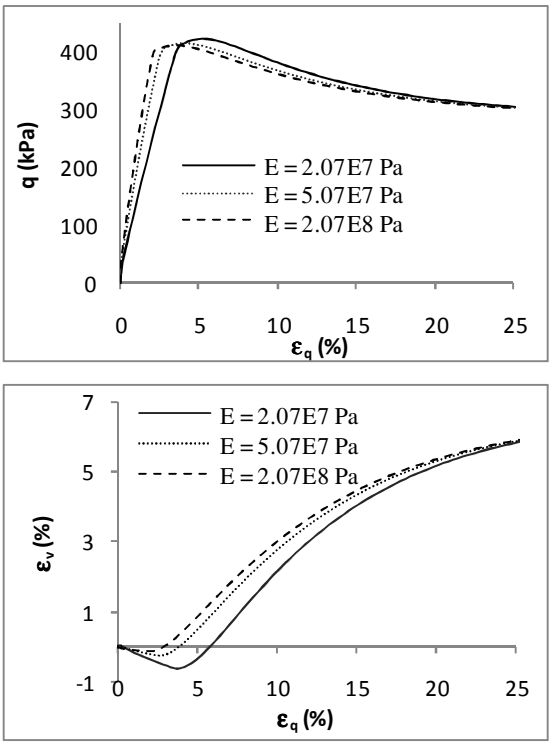

Figure 11. Schematic view of the model response with variation of Elastic Modulus

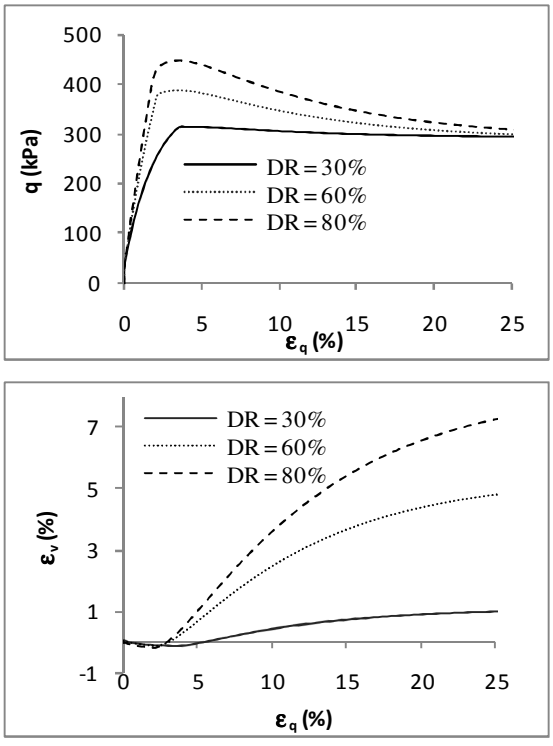

Figure 13. Schematic view of the model response with variation of relative density

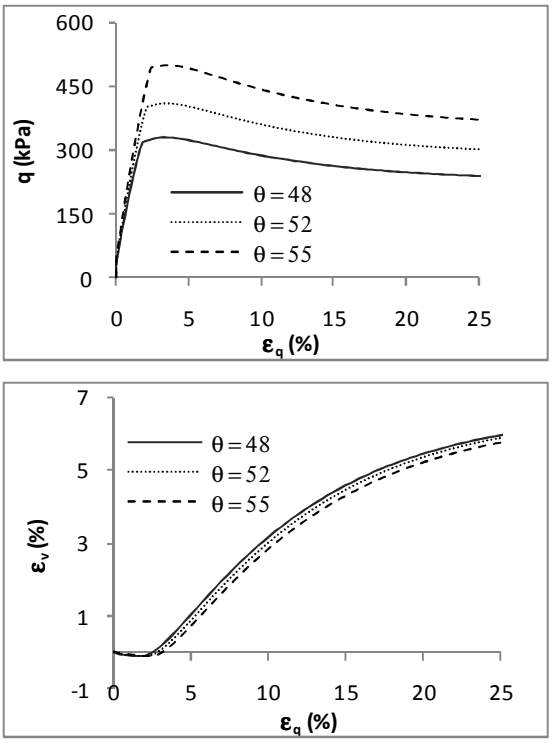

Figure 12. Schematic view of the model response with variation of angle of internal friction in *p'-q* space

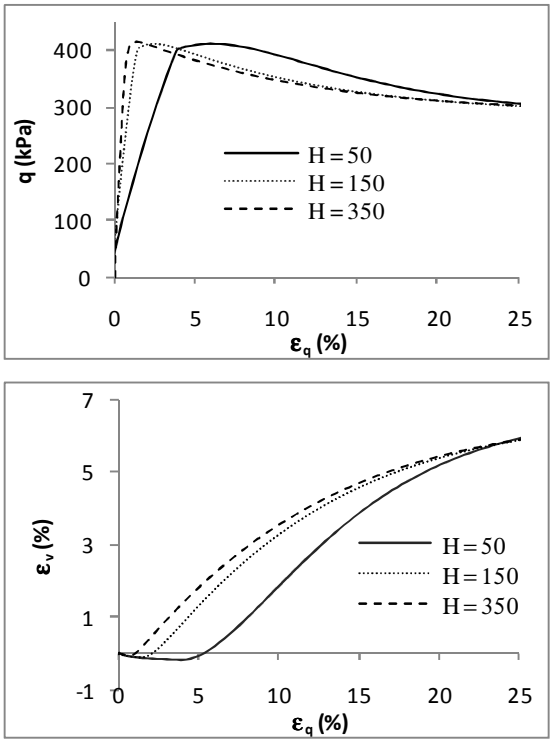

Figure 14. Schematic view of the model response with variation of hardening modulus

6 CONCLUSION

In this paper the Drucker-Prager Cap model was improved to capture different responses of sands depending on the initial density and stress level. The result is a simple model with 10 easy to determine parameters that can relatively accurately predicts the strain-stress behaviour of the soils. The proposed constitutive model can address the issue of excessive dilation of which the Drucker-Prager Cap model suffers. The excessive dilation is superseded by more realistic dilatancy rates through the application of dilatancy index proposed by Bolton (1986). The shear hardening law of the model which is based on soil state and a maximum allowable dilation enables the model to predict some of the dense sand behaviours such as softening.

In this study the proposed model has been validated for drained behaviour of loose to dense sand under triaxial condition.

The model has been implemented in ABAQUS FE software using a user defined subroutine VUMAT in order to simulate large strain behaviour of sand during ice gouging event. Through the application of volume constraint method, the model was also extended to predict the undrained behaviour of soils. The research is in progress for undrained condition.

REFERENCES

Been, K., & Jefferies, M. G. (1985). A state parameter for sands. *Geotechnique , 35* (2), 99-112.

Bolton, M. D. (1986). The strength and dilatancy of sands. *Geotechnique , 36* (1), 65-78.

Chakraborty, T., & Salgado, R. (2010). Dilatancy and Shear Strength of Sand at Low Confining Pressures. *J. Geotech. and Geoenvir. Engrg. , 136* (3), 527-532.

Cubrinovski, M., & Ishihara, K. (1998). Modelling of sand behaviour based on state concept. *Soils and Foundations , 38* (2), 115-127.

Drucker, D. C., & Prager, W. (1952). Soil mechanics and plastic analysis on limit design. *Q. Appl. Math , 10*, 157-165.

Drucker, D. C., Gibson, R. E., & Henkel, D. J. (1957). Soil mechanics and work hardening theories of plasticity. *J. Soil Mech. Fdn Engng Div. Am. Sot. Civ. , 122*, 338-346.

Ishihara, K. (1993). Liquefaction and flow failure during earthquakes. *Géotechnique , 43* (3), 351-415.

Jefferies, M. G. (1997). Plastic work and isotropic softening in unloading. *Geotechnique , 47* (5), 1037-1042.

Jefferies, M., & Been, K. (2006). *Soil Liquefaction.* Taylor & Francis.

Phillips, R., Barrett, J. & Al-Showaiter. A. (2010) Ice keel-seabed interaction: numerical modelling validation
Offshore Technology Conference, Paper OTC 20696

Roscoe, K. H., & Poorooshasb, H. B. (1963). A fundamental principle of similarity in model tests for earth pressure problems. *2nd Asian Conference on Soil Mechanics*, (pp. 134-140).

Verdugo, R. (1992). *Characterization of sandy soil behavior under large deformation.* Ph.D. thesis, University of Tokyo, Tokyo, Japan.

Vermeer, P. A., & de Borst, R. (1984). Non-associated plasticity for soils, concrete and rock. *Heron, 29, No. 3.*